ChemComm

COMMUNICATION

View Article Online
View Journal | View Issue



Cite this: *Chem. Commun.*, 2018, **54**, 6068

Received 28th April 2018,
Accepted 21st May 2018

DOI: 10.1039/c8cc03461c

rsc.li/chemcomm



# Tunable photo-luminescence behaviors of macrocycle-containing polymer networks in the solid-state†

Qian Zhao[a] and Yu Liu *[ab]

**Two porous polymers were synthesized from tetraphenylethylene (TPE) crosslinked β-cyclodextrins (β-CD) and sulfonatocalix[4]arene (SC4A). Owing to the FRET process from the TPE to the encapsulated fluorophores, these polymers provide universal platforms for the fabrication of photo-luminescence tunable organic solid materials.**

Tunable organic photo-luminescent materials, especially solid materials, have numerous applications including in optical memory devices, security materials, organic luminescent displays, fluorescent sensors and so on.[1] However, traditional organic luminogens, which possess planar structures, are weakly emissive or even non-emissive in their solid state due to the strong non-radiative decay aroused by intermolecular π–π stacking.[2] Compared with these aggregation-caused quenching (ACQ) luminogens, aggregation-induced emission luminogens (AIEgens) could give strong emissions with high quantum efficiency in the solid state.[3] Typical AIEgens are tetraphenylethylene derivatives (TPE), which possess a quadrilateral geometry and their rigid aromatic rings make them important building units in luminescent porous materials, such as metal–organic frameworks (MOFs),[4] covalent organic frameworks (COFs),[5] supramolecular organic frameworks (SOFs),[6] hydrogen-bonded organic frameworks (HOFs)[7] and porous polymers.[8] Although these porous materials can encapsulate small molecules, the encapsulated fluorophores (EFs) often have π–π interactions with the aromatic moieties in the porous materials, which results in fluorescence quenching through intermolecular electron transfer or charge transfer processes (Fig. 1a).[4a,9] Therefore, a lot of effort has been dedicated to the fabrication of porous organic solid materials with tunable photo-luminescence properties.[10] An usual strategy is to crosslink two kinds of fluorescent moieties to extended skeletons without π–π stacking, but it is hard to regulate the emission colors because the fluorophores have already been fixed.[10c] Recently, Jiang and Hu *et al.* have synthesized fluorescent porous polymers, which allowed emission color regulation between the polymers and the encapsulated fluorophores *via* FRET.[11] However, in the aforementioned porous materials, the pores for encapsulating fluorophores were bound by the crosslinked fluorescent moieties, so the special shapes of the pores were crucial for preventing the π–π interactions, which greatly rely on elaborate fabrication and sometimes on an accidental discovery.

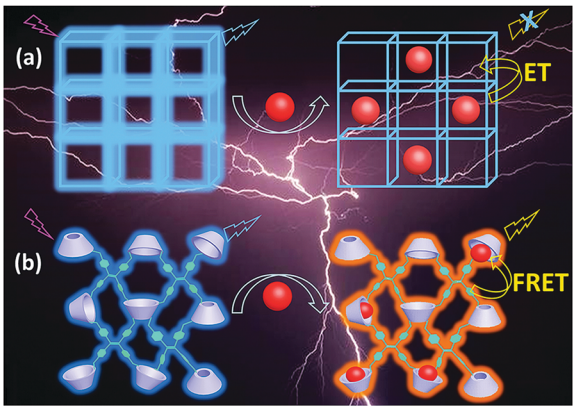


Fig. 1 Schematic illustration of (a) fluorescent porous materials encapsulating small molecules resulting in fluorescence quenching through an ET process; (b) fluorescent porous materials based on macrocycles binding dyes with FRET induced emission color tuning.

It is well known that macrocycles such as cyclodextrin or calix[4]arene (cyclic oligomers formed by the linkage of glucoses or phenols) have specific pore structures and selective binding abilities, and they have been widely applied in adsorptions and separations for dyes.[12] Therefore, macrocycles may be the best choices for fabricating tunable solid state photo-luminescent materials. Herein, we report two porous organic solid materials based on TPE crosslinked macrocycles, cyclodextrins (CDs) and sulfonatocalix[4]arene (SC4A), which could conveniently tune the emission colors from blue-green to red-orange *via* efficient FRET from TPE to EFs. These results indicate that the

[a] *College of Chemistry, State Key Laboratory of Elemento-Organic Chemistry, Nankai University, Tianjin 300071, P. R. China. E-mail: yuliu@nankai.edu.cn*
[b] *Collaborative Innovation Center of Chemical Science and Engineering (Tianjin), Nankai University, Tianjin 300071, P. R. China*

† Electronic supplementary information (ESI) available. See DOI: 10.1039/c8cc03461c

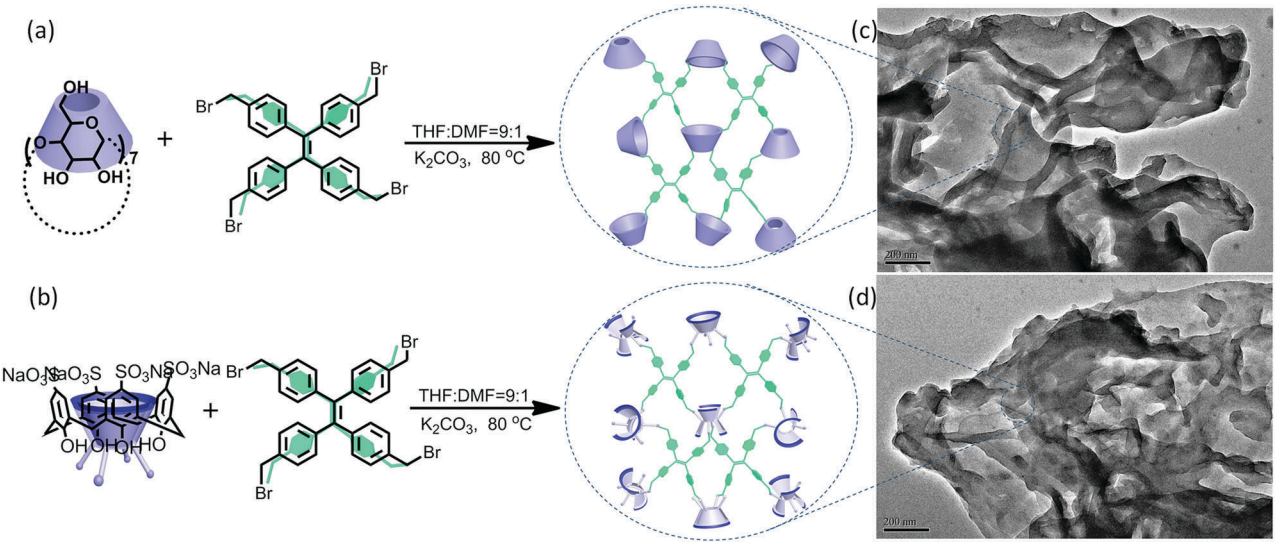


Fig. 2 Synthetic routes of (a) TPECD and (b) TPESC4A polymers in a mixture of THF and DMF; TEM images of (c) TPECD and (d) TPESC4A polymers.

fluorophore@AIEgen crosslinked macrocycles are universal platforms for the fabrication of photo-luminescence-tunable organic materials in the solid state.

β-CD and SC4A were crosslinked by tetrakis(4-(bromomethyl)-phenyl)ethane (TPEBr) *via* the nucleophilic substitution of the hydroxyl groups on the macrocycles, and the corresponding TPE crosslinked β-CD polymers (TPECD) or TPE crosslinked SC4A polymers (TPESC4A) were formed, respectively (Fig. 2a and b). Then, these TPECD and TPESC4A polymers were subjected to a series of characterizations. As shown in the solid-state $^{13}$C NMR spectrum of the TPECD polymer (Fig. S1, ESI†), the resonance peaks at $\delta$ 51.2 and 78.5 ppm were associated with β-CD, and the peaks at 131.9 and 142.1 ppm corresponded to the TPE moiety, suggesting the integration of β-CD and TPE. Similarly, in the solid-state $^{13}$C NMR spectrum of the TPESC4A polymer (Fig. S2, ESI†), the peaks at $\delta$ 51.1 and 47.2 ppm were associated with the SC4A(–$CH_2$–), and the peaks at $\delta$ 70.5 and 65.1 ppm corresponded to the TPE(–$CH_2$–) unit, indicating the combination of SC4A and TPE. Also, IR was used to demonstrate the formation of ether bonds (Fig. S3–S6, ESI†) and TG was exploited to characterize the thermal stability of the two macrocycle-containing polymers (Fig. S7–S10, ESI†).

The combination of TPE and β-CD/SC4A endowed the polymers with many excellent qualities such as good water-dispersible ability and solid luminescence capability. As shown in Fig. S11 and S12 (ESI†), the solid fluorescence excitation and emission spectra of TPECD/TPESC4A presented their maximum absorbance and emission intensity both at about 350 nm and 500 nm, respectively, suggesting their potential application as solid-state light emitting materials. Samples prepared from the suspension of polymers were observed by TEM (Fig. 2c and d) and SEM (Fig. S13 and S14, ESI†). We can clearly see that the samples consist exclusively of layered nanosheets, which are curved and to some extent interconnected by the TEM images. Identical morphologies were also observed by SEM, presenting a very loosely packed architecture indicating well its adsorption capacity.[12b] So, $N_2$ adsorption and

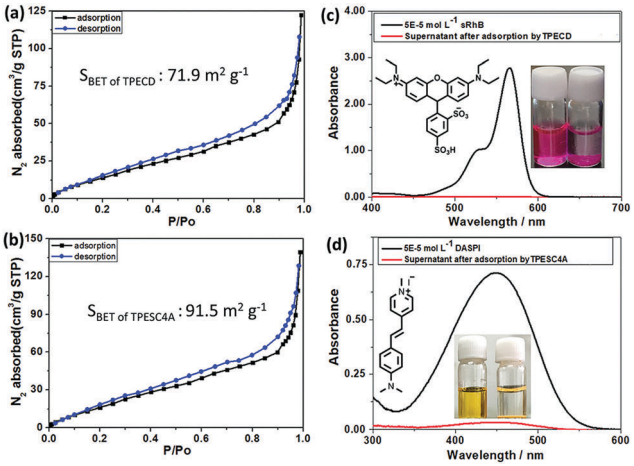


Fig. 3 $N_2$ adsorption (blue line) and desorption (black line) isotherms of (a) TPECD and (b) TPESC4A polymers (the solid line is a guide to the eye. $S_{BET}$ is the Brunauer–Emmett–Teller (BET) surface area (in units of $m^2\ g^{-1}$) of the TPECD and TPESC4A polymers calculated from the $N_2$ adsorption isotherm, and $P$ and $P_0$ are the equilibrium and saturation pressures of $N_2$ at 77 K, respectively); UV-Vis spectra of the dyes (50 μM) before (black) and after (red) adsorption with (c) TPECD and (d) TPESC4A polymer (1 mg of polymer with 1 mL of 50 μM dye solution for 5 minutes) (inset pictures: structures of the dyes, and photos of the solution before and after adsorption by the polymers).

desorption experiments were done to detect the surface areas and porosimetry of the TPECD and TPESC4A polymer. The Brunauer–Emmett–Teller ($S_{BET}$) surface areas of the TPECD and TPESC4A (Fig. 3a and b) polymers were calculated as 71.9 $m^2\ g^{-1}$ and 91.5 $m^2\ g^{-1}$ *via* the multi-point BET method,[13] which are much higher than the β-CD polymer crosslinked with epichlorohydrin ($S_{BET}$ = 23 $m^2\ g^{-1}$), the most extensively investigated β-CD polymer for water purification, which has already been commercialized.[12b,14] The BJH method[15] applied to the isotherm curves indicated that the majority of pore sizes concentrated at 2.75 nm for the TPECD polymer (Fig. S15, ESI†) and 2.74 nm for the TPESC4A polymer (Fig. S16, ESI†). The XRD patterns of both

polymers (Fig. S17 and S18, ESI†) showed large broad diffraction peaks, indicating a low degree of crystallinity due to the random cross linkages.

The experiments for the adsorption of dyes were done using these porous polymers. From the UV-Vis absorbance of sulforhodamine B (sRhB, 50 μM) and the supernatant of sRhB (50 μM)@TPECD (1 mg $mL^{-1}$), we can see that sRhB can be completely adsorbed by TPECD (Fig. 3c). Also the inset photograph in Fig. 3c demonstrates that sRhB with an initial concentration of 50 μM is completely removed from water by TPECD after 4 minutes (Fig. S19–S22, ESI†). The maximum uptake capability for sRhB was measured as 68 μmol $g^{-1}$ (Fig. S23 and S24, ESI†). At the same time, adsorption towards eight other sulfonatophenyl dyes (50 μM) was measured, which can be completely removed by TPECD (1 mg $mL^{-1}$) (Fig. S25–S32, ESI†). The adsorption of dyes with the sulfonatophenyl functional group could be attributed to the excellent binding ability of CD with anionic dyes.[16] Meanwhile, the ionic dyes often gave high binding affinities to SC4A. As shown in the inset photograph of Fig. 3d, the color of the aqueous 4-[4-(dimethylamino)styryl]-1-methylpyridinium iodide (DASPI, 50 μM) solution disappeared upon addition of TPESC4A (1 mg $mL^{-1}$) after 4 minutes (Fig. S33–S36, ESI†). Also, the absorption peak of a DASPI solution at around 450 nm decreased significantly to less than 3% of its original absorbance in the presence of the TPESC4A polymer, suggesting that DASPI was well adsorbed on TPESC4A due to the strong complexation between DASPI and SC4A.[17] We titrated the TPESC4A polymers with different amounts of DASPI and determined the maximum uptake capability as 59 μmol $g^{-1}$ (Fig. S37 and S38, ESI†).

DASPI is a classic molecule with intramolecular charge transfer from the *N*,*N*-diethylamino moiety to the *p*-methoxyl phenyl group, the emission of which can be greatly enhanced when it is located in a confined region due to the suppression of twisted intramolecular charge transfer (TICT) effect.[18] So the strong adsorption of DASPI on TPESC4A enabled us to tune the emission colors from blue-green to red-orange by simply changing the adsorbed amount of DASPI, and this luminescence behavior was confirmed by the photos of pTPESC4A and DASPI@pTPESC4A taken under natural light and 365 nm light (Fig. 4a). A series of homogeneous DASPI@TPESC4A powders from 0–40 μmol $g^{-1}$ were subjected to solid phase fluorescence spectroscopy. When excited at 365 nm, two peaks around 500 and 580 nm in the fluorescence spectra were assignable to the components TPESC4A and DASPI, respectively (Fig. 4b). As the absorbed amount of DASPI increased, the fluorescence peaks of DASPI@TPESC4A at 500 nm decreased significantly and the peaks around 580 nm increased rapidly along with more than 20 nm fluorescence shift from 567 nm to 590 nm. The trajectory of the color changes based on the fluorescence spectra of DASPI@TPESC4A was marked out on a CIE program (Fig. 4c) which was in good agreement with the photos taken under 365 nm light (Fig. 4a). The excitation spectrum of DASPI overlapped well with the fluorescence band of TPESC4A (Fig. 4d). Compared to no emission of DASPI, the strong emission of DASPI@TPESC4A (Fig. S39, ESI†) indicated the FRET[8c,19] from TPESC4A to DASPI. The efficiency of energy transfer ($\Phi_{ET}$) calculated for DASPI@TPESC4A (40 μmoL $g^{-1}$) is 87% according to the fluorescence spectra (Fig. S40, ESI†). The fluorescence decay of TPESC4A (Fig. S41, ESI†) was fitted by two exponential components $\tau$1 2.26 ns (47%) and $\tau$2 7.78 ns (53%). Such bi-exponential decays could be attributed to the inhomogeneous surrounding environment of the TPE group[8c] and the

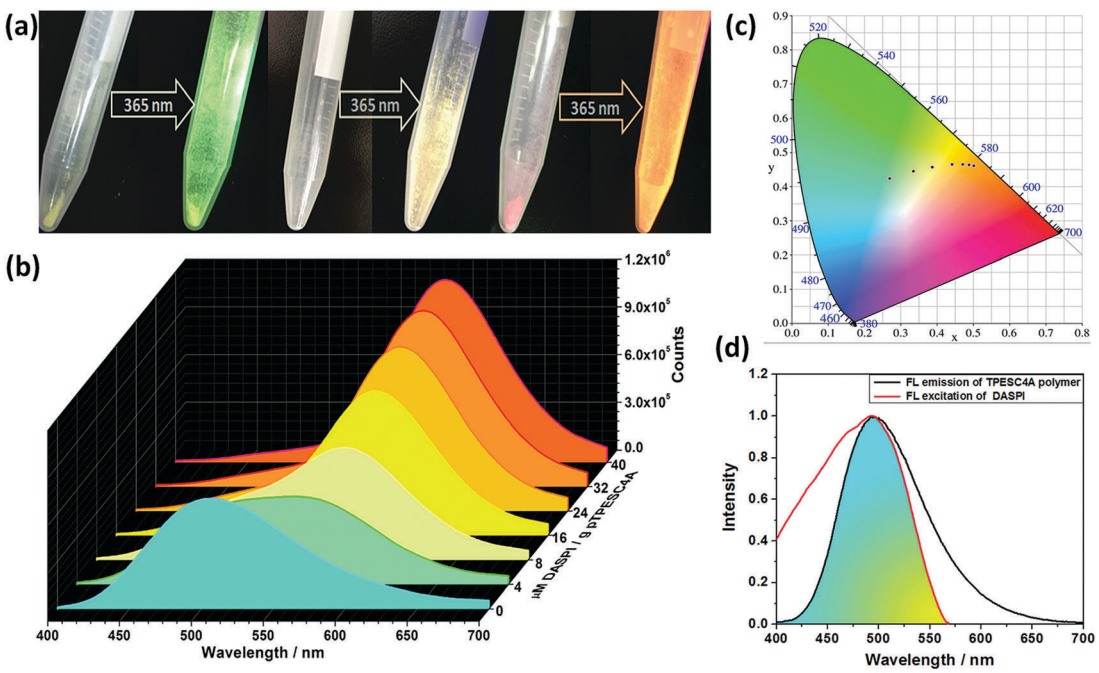


Fig. 4 (a) Photos of TPESC4A and DASPI@TPESC4A taken under natural light and 365 nm light; (b) fluorescence emission spectra of DASPI@TPESC4A (0, 4, 8, 16, 24, 32 and 40 μmol $g^{-1}$ from front to back); (c) CIE diagram showing the trajectory of the color changes; (d) overlap of the excitation spectrum of DASPI and the fluorescence band of the TPESC4A polymer.

 

average lifetime calculated as 5.17 ns could be considered to make meaningful sense out of the data. The fluorescence decays at different wavelengths of DASPI@TPESC4A (40 μmol $g^{-1}$) were also best fitted with bi-exponential terms, owing to the two excited states of DASPI, the local excited state and TICT state (Fig. S42–S47 and Table S1, ESI†).[18a] Experiments were also done using sRhB@TPECD and similar phenomena were observed. An increasing amount of sRhB resulted in the peak at 500 nm gradually being quenched together with a 10 nm bathochromic shift and the peak at 583 nm increased slowly with a 10 nm hypochromic shift (Fig. S48, ESI†). The trajectory of the color changes based on the spectra of sRhB@TPECD was marked out on a CIE program (Fig. S49, ESI†), which was in good agreement with the photos taken under 365 nm light (Fig. S50, ESI†). The absorption band of sRhB showed a good overlap with the fluorescence band of TPECD ranging from 460 to 600 nm (Fig. S51, ESI†). Compared to the emission of sRhB@TPECD, sRhB itself did not emit (Fig. S52, ESI†), which ruled out the possibility of the direct excitation of the acceptor, indicating the FRET process from TPECD to sRhB. $\Phi_{ET}$ was calculated as 68% when the adsorption of sRhB on TPECD was 50 μmol $g^{-1}$ (Fig. S53, ESI†). Furthermore, when TPECD or sRhB@TPECD was blended with poly(vinyl alcohol) (PVA) aqueous solution (10 wt%), a series of homogeneous, transparent and brightly luminescent films were obtained (Fig. S56, blue-green and orange were corresponding to TPECD and sRhB@TPECD respectively, ESI†). The average lifetime of TPECD was 2.65 ns and a single lifetime 2.69 ns was fitted for sRhB@TPECD (50 μmol $g^{-1}$) (Fig. S54 and S55, ESI†).

In summary, two crosslinked mesoporous polymers based on macrocycles (β-CD and SC4A) and TPE have certain absorption capacities for different corresponding fluorophores (sRhB and DASPI) due to efficient host–guest complexations. The supramolecular inclusion of sRhB and DASPI by macrocycles in the polymers made these fluorophores spatially separate with the TPE moieties, so that FRET could occur between TPE and sRhB/DASPI. The $\Phi_{ET}$ of DASPI@TPESC4A was 87% which is bigger than the $\Phi_{ET}$ of sRhB@TPECD (68%), partly because the overlap between the fluorescence of TPE and the excitation spectrum of DASPI is better than the overlap between TPE and sRhB. These two different FRETs from crosslinked macrocyclic host polymers to fluorescent guests proved that our strategy was an effective way of tuning the solid photo-luminescence by simple changes of the adsorbed amount of fluorophores. We do believe that these platforms based on fluorophore@AIEgen crosslinked macrocycles are efficient and convenient for the fabrication of photo-luminescence-tunable solid organic materials in various forms.

Financial support from the National Natural Science Foundation of China (21432004 and 91527301) is acknowledged.

## Conflicts of interest

The authors have no conflicts of interest to declare for this communication.

## Notes and references

1 (*a*) S. Baysec, E. Preis, S. Allard and U. Scherf, *Macromol. Rapid Commun.*, 2016, **37**, 1802–1806; (*b*) B. W. D'Andrade and S. R. Forrest, *Adv. Mater.*, 2004, **16**, 1585–1595; (*c*) H. Dong, C. Zhang, Y. Liu, Y. Yan, F. Hu and S. Zhao Yong, *Angew. Chem., Int. Ed.*, 2018, **57**, 3108–3112; (*d*) X. Hou, C. Ke, C. J. Bruns, P. R. McGonigal, R. B. Pettman and J. F. Stoddart, *Nat. Commun.*, 2015, **6**, 6884–6892; (*e*) N. Kalluvettukuzhy, S. Pagidi, D. Kumbhar and P. Thilagar, *Chem. Commun.*, 2016, **53**, 3641–3644; (*f*) D. Li, F. Lu, J. Wang, W. Hu, X.-M. Cao, X. Ma and H. Tian, *J. Am. Chem. Soc.*, 2018, **140**, 1916–1923; (*g*) J. Liu, Y. Zhuang, L. Wang, T. Zhou, N. Hirosaki and R.-J. Xie, *ACS Appl. Mater. Interfaces*, 2018, **10**, 1802–1809; (*h*) T. Mutai, H. Satou and K. Araki, *Nat. Mater.*, 2005, **4**, 685–687; (*i*) J. N. Zhang, H. Kang, N. Li, S. M. Zhou, H. M. Sun, S. W. Yin, N. Zhao and B. Z. Tang, *Chem. Sci.*, 2017, **8**, 577–582.

2 J. B. Birks, *Photophysics of Aromatic Molecules*, Wiley, London, 1970.

3 (*a*) R. Hu, N. L. C. Leung and B. Z. Tang, *Chem. Soc. Rev.*, 2014, **43**, 4494–4562; (*b*) J. Mei, N. L. C. Leung, R. T. K. Kwok, J. W. Y. Lam and B. Z. Tang, *Chem. Rev.*, 2015, **115**, 11718–11940; (*c*) Q. Zhao, Y. Chen and Y. Liu, *Chin. Chem. Lett.*, 2018, **29**, 84–86; (*d*) Q. Zhao, Y. Chen, M. Sun, X.-J. Wu and Y. Liu, *RSC Adv.*, 2016, **6**, 50673–50679.

4 (*a*) Z. Hu, W. P. Lustig, J. Zhang, C. Zheng, H. Wang, S. J. Teat, Q. Gong, N. D. Rudd and J. Li, *J. Am. Chem. Soc.*, 2015, **137**, 16209–16215; (*b*) Q. Zhang, J. Su, D. Feng, Z. Wei, X. Zou and H.-C. Zhou, *J. Am. Chem. Soc.*, 2015, **137**, 10064–10067; (*c*) X. Zhao, X. Song, Y. Li, Z. Chang and L. Chen, *ACS Appl. Mater. Interfaces*, 2018, **10**, 5633–5640.

5 (*a*) S. Dalapati, E. Jin, M. Addicoat, T. Heine and D. Jiang, *J. Am. Chem. Soc.*, 2016, **138**, 5797–5800; (*b*) Z.-F. Pang, S.-Q. Xu, T.-Y. Zhou, R.-R. Liang, T.-G. Zhan and X. Zhao, *J. Am. Chem. Soc.*, 2016, **138**, 4710–4713.

6 S.-Q. Xu, X. Zhang, C.-B. Nie, Z.-F. Pang, X.-N. Xu and X. Zhao, *Chem. Commun.*, 2015, **51**, 16417–16420.

7 (*a*) Y. Lin, X. Jiang, S. T. Kim, S. B. Alahakoon, X. Hou, Z. Zhang, C. M. Thompson, R. A. Smaldone and C. Ke, *J. Am. Chem. Soc.*, 2017, **139**, 7172–7175; (*b*) T. Yu, D. Ou, Z. Yang, Q. Huang, Z. Mao, J. Chen, Y. Zhang, S. Liu, J. Xu, M. R. Bryce and Z. Chi, *Chem. Sci.*, 2017, **8**, 1163–1168.

8 (*a*) S. Dalapati, C. Gu and D. Jiang, *Small*, 2016, **12**, 6513–6527; (*b*) K. Yuan, P. Guo-Wang, T. Hu, L. Shi, R. Zeng, M. Forster, T. Pichler, Y. Chen and U. Scherf, *Chem. Mater.*, 2015, **27**, 7403–7411; (*c*) P. Zhang, K. Wu, J. Guo and C. Wang, *ACS Macro Lett.*, 2014, **3**, 1139–1144.

9 (*a*) L. E. Kreno, K. Leong, O. K. Farha, M. Allendorf, R. P. Van Duyne and J. T. Hupp, *Chem. Rev.*, 2012, **112**, 1105–1125; (*b*) Y. Zhang, S. Yuan, G. Day, X. Wang, X. Yang and H.-C. Zhou, *Coord. Chem. Rev.*, 2018, **354**, 28–45.

10 (*a*) Y. Cui, Y. Yue, G. Qian and B. Chen, *Chem. Rev.*, 2012, **112**, 1126–1162; (*b*) K. Müller-Buschbaum, F. Beuerle and C. Feldmann, *Microporous Mesoporous Mater.*, 2015, **216**, 171–199; (*c*) X. Zhang, W. Wang, Z. Hu, G. Wang and K. Uvdal, *Coord. Chem. Rev.*, 2015, **284**, 206–235.

11 (*a*) S. Bi, Y. Li, L. Wang, J. Hu and H. Liu, *J. Phys. Chem. C*, 2017, **121**, 6685–6691; (*b*) L. Chen, Y. Honsho, S. Seki and D. Jiang, *J. Am. Chem. Soc.*, 2010, **132**, 6742–6748.

12 (*a*) E. Akceylan, M. Bahadir and M. Yılmaz, *J. Hazard. Mater.*, 2009, **162**, 960–966; (*b*) A. Alsbaiee, B. J. Smith, L. Xiao, Y. Ling, D. E. Helbling and W. R. Dichtel, *Nature*, 2016, **529**, 190–194; (*c*) M. Chen, T. Shang, W. Fang and G. Diao, *J. Hazard. Mater.*, 2011, **185**, 914–921; (*d*) M. A. Kamboh, I. B. Solangi, S. T. H. Sherazi and S. Memon, *Desalination*, 2011, **268**, 83–89; (*e*) P. Lo Meo, G. Lazzara, L. Liotta, S. Riela and R. Noto, *Polym. Chem.*, 2014, **5**, 4499–4510.

13 K. Yang and B. Xing, *Environ. Pollut.*, 2009, **157**, 1095–1100.

14 H. Liu, X. Cai, Y. Wang and J. Chen, *Water Res.*, 2011, **45**, 3499–3511.

15 J. C. Yu, J. Yu, W. Ho and L. Zhang, *Chem. Commun.*, 2001, 1942–1943.

16 (*a*) T. Iijima and Y. Karube, *Dyes Pigm.*, 1998, **36**, 305–311; (*b*) L. Li, P. Liang and Y. Liu, *Chin. Chem. Lett.*, 2003, **14**, 9–12.

17 S. Fernández-Abad, M. Pessêgo, N. Basílio and L. García-Río, *Chem. – Eur. J.*, 2016, **22**, 6466–6470.

18 (*a*) H. Dong, Y. Wei, W. Zhang, C. Wei, C. Zhang, J. Yao and Y. S. Zhao, *J. Am. Chem. Soc.*, 2016, **138**, 1118–1121; (*b*) Z. R. Grabowski, K. Rotkiewicz and W. Rettig, *Chem. Rev.*, 2003, **103**, 3899–4032; (*c*) Y.-M. Zhang, X.-J. Zhang, X. Xu, X.-N. Fu, H.-B. Hou and Y. Liu, *J. Phys. Chem. B*, 2016, **120**, 3932–3940; (*d*) Q. Zhao, Y. Chen, S.-H. Li and Y. Liu, *Chem. Commun.*, 2018, **54**, 200–203.

19 M. Zhang, X. Yin, T. Tian, Y. Liang, W. Li, Y. Lan, J. Li, M. Zhou, Y. Ju and G. Li, *Chem. Commun.*, 2015, **51**, 10210–10213.